

Density-functional calculations of the electronic structure and lattice dynamics of superconducting $\text{LaO}_{0.5}\text{F}_{0.5}\text{BiS}_2$: Evidence for an electron-phonon interaction near the charge-density-wave instability

Xiangang Wan,^{1,3} Hang-Chen Ding,² Sergey Y. Savrasov³ and Chun-Gang Duan^{2,4}

¹*National Laboratory of Solid State Microstructures and Department of Physics, Nanjing University, Nanjing 210093, China*

²*Key Laboratory of Polar Materials and Devices, Ministry of Education, East China Normal University, Shanghai 200062, China*

³*Department of Physics, University of California, Davis, One Shields Avenue, Davis, CA 95616, USA*

⁴*National Laboratory for Infrared Physics, Chinese Academy of Sciences, Shanghai 200083, China*

(Dated: June 18, 2018)

We discuss the electronic structure, lattice dynamics and electron–phonon interaction of newly discovered superconductor $\text{LaO}_{0.5}\text{F}_{0.5}\text{BiS}_2$ using density functional based calculations. A strong Fermi surface nesting at $\mathbf{k}=(\pi,\pi,0)$ suggests a proximity to charge density wave instability and leads to imaginary harmonic phonons at this \mathbf{k} point associated with in–plane displacements of S atoms. Total energy analysis resolves only a shallow double-well potential well preventing the appearance of static long–range order. Both harmonic and anharmonic contributions to electron–phonon coupling are evaluated and give a total coupling constant $\lambda \simeq 0.85$ prompting this material to be a conventional superconductor contrary to structurally similar FeAs materials.

PACS numbers: 74.20.Pq, 74.70.-b

Superconductors with layered crystal structures such as cuprates[1], ruthenates[2], or MgB_2 [3] have generated enormous research interest. A recent discovery of iron pnictides[4] have triggered another wave of extensive studies [5], and while the mediator of pairing in these systems remains officially unidentified, a large amount of evidence points to magnetic spin fluctuations induced by antiferromagnetic spin–density–wave (SDW) instability due to Fermi–surface nesting[6] at wave vector $\mathbf{k}=(\pi,\pi,0)$ similar to the cuprates. Usually changing the blocking layer can tune the superconducting T_c , thus searching for new layered superconductors is of both fundamental and technological importance.

Very recently, a new layered superconductor $\text{Bi}_4\text{O}_4\text{S}_3$ has been found[7], and soon after, two other systems, $\text{LaO}_{1-x}\text{F}_x\text{BiS}_2$ [1] and NdOBiS_2 [9] have been discovered. Here, the basic structural unit is the BiS_2 layer which is similar to the Cu–O planes in Cu–based superconductors[1] and the Fe–A (A=P, As, Se, Te) planes in iron pnictides[5]. A chance to explore superconductivity and increase T_c in these new compounds has already resulted in a lot of work that appeared shortly after the discovery[1, 7, 9–16]. Hall effect measurements reveal multiband features and suggest the superconducting pairing occurs in one–dimensional chains [10]. It was proposed that these compounds are type II superconductors and good candidates for thermoelectric materials [11]. Electrical resistivity measurements under pressure reveal that $\text{Bi}_4\text{O}_4\text{S}_3$ and $\text{La}(\text{O},\text{F})\text{BiS}_2$ have different T_c versus pressure behavior, and the Fermi surface of $\text{La}(\text{O},\text{F})\text{BiS}_2$ may be located in the vicinity of some instabilities[12]. A two p bands electronic model has been proposed based on band structure calculation[13], and a

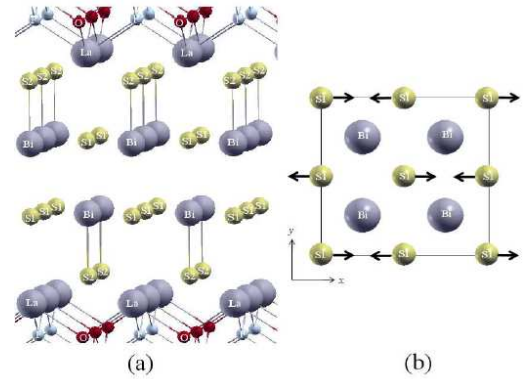


FIG. 1: (a) Structure of $\text{La}(\text{O}_{0.5}\text{F}_{0.5})\text{BiS}_2$; (b) unstable phonon mode corresponding to wave vector $\mathbf{k}=(\pi,\pi,0)$.

good Fermi–surface nesting with wave vector $\mathbf{k}=(\pi,\pi,0)$ has been found[13]. The importance of the nesting has been emphasized experimentally[12] and it was suggested that electronic correlations may play a role in superconductivity of these systems [14].

Here we report our theoretical studies of the electronic structure and lattice dynamic properties for $\text{LaO}_{0.5}\text{F}_{0.5}\text{BiS}_2$, the compound that possesses the highest $T_c \simeq 10$ K [1] among known BiS based materials[1, 7, 9] and whose structure is similar to superconducting iron arsenides $\text{LaFeO}_{1-x}\text{F}_x\text{As}$ [4]. Our first–principles calculations are based on density functional theory (DFT) and show that the bands around the Fermi level are not sen-

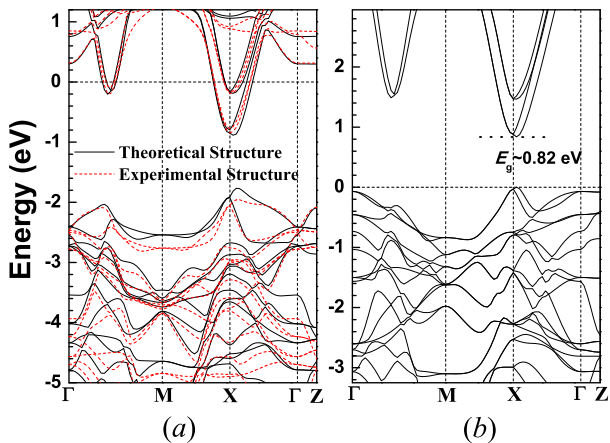


FIG. 2: Band structure of (a) $\text{LaO}_{0.5}\text{F}_{0.5}\text{BiS}_2$; (b) LaOBiS_2 .

sitive to F substitution, thus making rigid band approximation adequate for $\text{LaO}_{1-x}\text{F}_x\text{BiS}_2$. We find a strong nesting of the Fermi surface at $\mathbf{k} = (\pi, \pi, 0)$ for $x=0.5$ by performing the calculation for ordered compound $\text{LaO}_{0.5}\text{F}_{0.5}\text{BiS}_2$. Our linear response based phonon calculation shows that the nesting results in a large phonon softening at this \mathbf{k} and in the appearance of the imaginary modes associated with in-plane displacements of S atoms. Our $\sqrt{2} \times \sqrt{2} \times 1$ supercell total-energy calculation finds a shallow double-well potential prompting that these displacements are dynamic. Contrary to the expectations that electronic correlations may play a role in these systems, our calculated electron-phonon coupling constant $\lambda \simeq 0.85$ suggests that this material is a conventional superconductor. However, our anharmonic model calculation shows that the vicinity of the charge-density-wave (CDW) instability is essential for the superconductivity which is reminiscent to iron pnictides whose proximity to SDW is well established[4].

Our electronic structure calculations are performed within the generalized gradient approximation (GGA)[17]. Whenever possible, we cross-check the results by two different commonly used total-energy codes: a) the Vienna Ab-Initio Simulation Package (VASP)[18] and b) the Quantum ESPRESSO package (QE)[19]. The consistency of our results for two sets of calculations is satisfactory. We use a 500 eV plane-wave cutoff and a dense $18 \times 18 \times 6$ k-point mesh in the irreducible Brillouin zone (IBZ) for self-consistent calculations. For structural optimization, the positions of ions were relaxed towards equilibrium until the Hellman-Feynman forces became less than 2 meV/Å. For the phonon calculations, we adopt a scalar relativistic version of density-functional linear-response method[20] as implemented in QE[19]. For consistency, the results presented in this paper are obtained by scalar relativistic version of QE, unless otherwise specified. The effect of spin-orbit coupling (SOC) is discussed in

TABLE I: Calculated lattice parameters and Wyckoff positions of LaOBiS_2 and $\text{La}(\text{O}_{0.5}\text{F}_{0.5})\text{BiS}_2$. Experimental results [1] are also listed for comparison.

	LaOBiS_2		$\text{La}(\text{O}_{0.5}\text{F}_{0.5})\text{BiS}_2$		
	Site	Cal.	Exp.	Exp.	
a (Å)		4.0394	–	4.0780	4.0527
c (Å)		14.1232	–	13.4925	13.3237
z	La (2b)	0.0889	–	0.1049	0.1015
z	Bi (2b)	0.6304	–	0.6141	0.6231
z	S1 (2b)	0.3932	–	0.3902	0.3657
z	S2 (2b)	0.8090	–	0.8134	0.8198
z	O (2a)	0.0000	–	0.0000	0.0000
z	F (2a)	–	–	0.0000	0.0000

the Supplemental Material.

Powder x-ray diffraction (XRD) pattern shows that $\text{LaO}_{1-x}\text{F}_x\text{BiS}_2$ forms a layered crystal structure with a space group $P4/nmm$ [1]. La, S and Bi locate at 2b position, while O/F take the 2a site. Similar to $\text{LaO}_{1-x}\text{F}_x\text{FeAs}$ [4], the structure consists of alternating $\text{La}(\text{O}_{1-x}\text{F}_x)$ and BiS_2 layers[1]. One BiS_2 layer contains two BiS planes (namely Bi-S1 plane) and two pure S planes (i.e. S2 plane) as shown in Fig.1a. To study the influence of F doping, we carried out calculations for two systems, i.e. LaOBiS_2 ($x=0$) and $\text{LaO}_{0.5}\text{F}_{0.5}\text{BiS}_2$ ($x=0.5$). Being embedded into LaO plane, we expect that the substitution by F has only small effect on the BiS_2 layer. Thus we simulate $\text{LaO}_{0.5}\text{F}_{0.5}\text{BiS}_2$ by replacing half of the Oxygen 2a-sites by F orderly, despite the substitution may be random in reality. The optimized lattice parameters and Wyckoff positions for each atom are shown in Table I, together with available experimental data [1]. While the overall agreement between numerical and experimental structures is good, Table I reveals an interesting aspect: the differences between the experimental and theoretical values of the z -coordinate of S1 are unusually large, similar as in the FeAs-superconductors[21]. There is also a large difference between the numerical and experimental inter-layer distance. Note that we have also performed the internal atomic coordinates optimization based on the experimental lattice parameters (shown in the Table 1S of Supplementary Information). As can be seen from Table 1S of Supplementary Information, the lattice parameters, namely the inter-layer distance has only small effect on the z -coordinate of S1. In Table I we also list the numerical data for LaOBiS_2 . Comparing with the results for $\text{LaO}_{0.5}\text{Bi}_{0.5}\text{S}_2$, one can conclude that F substitution has only little effect on the lattice parameters, and a small effect on the BiS_2 layer.

The discrepancy between the experimental and theoretical positions of S1 atoms results in a considerable difference for valence band as shown in Fig.2a. We also perform calculation based on the numerical internal atomic coordinates and experimental lattice parameters. Com-

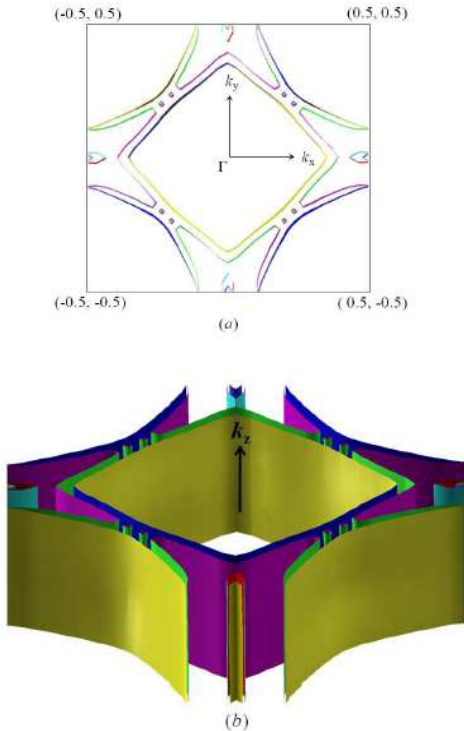


FIG. 3: Calculated Fermi surface of $\text{La}(\text{O}_{0.5}\text{F}_{0.5})\text{BiS}_2$: (a) cross section for $k_z=0$, (b) 3D view.

paring with the results based on theoretical structure shows that changing inter-layer distance only slightly affects the band structure, and the considerable difference shown in Fig.2a is mainly due to z -coordinate of S1. For LaOBiS_2 both S $3p$ and O $2p$ states appear mainly between -4.0 and 0.0 eV. Although located primarily above the Fermi level, Bi $6p$ have also a considerable contribution to the states between -4.0 and 0.0 eV, indicating a strong hybridization between Bi $6p$ and S $3p$ states. In agreement with previous calculation[13] our results show that LaOBiS_2 is an insulator with a band gap of 0.82 eV. A little dispersion along Γ to Z line clearly shows a two dimensional character of the band structure which indicates that the interlayer hybridization is small. Comparing Fig.2a and Fig.2b, it is clear that the main influence of F substitution is a carrier doping characterized by the associated upshift of the Fermi level towards the Bi $6p$ band, and the system becomes metallic as shown in Fig.2a. It is interesting to notice that doping by F has a negligible effect on the lowest conduction band. Thus we conclude that rigid band approximation is valid for $\text{LaO}_{1-x}\text{F}_x\text{BiS}_2$.

There are four bands that cross the Fermi level and result in a large two dimensional-like Fermi surface that is shown in Fig. 3. Consistent with the tight-binding

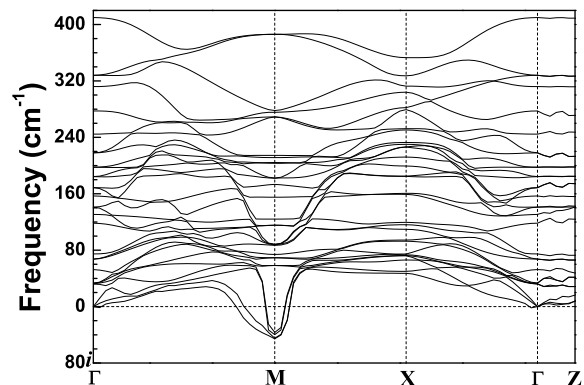


FIG. 4: Calculated phonon dispersions for $\text{LaO}_{0.5}\text{F}_{0.5}\text{BiS}_2$ using density functional linear response approach.

result[13], our density functional calculation shows a strong Fermi surface nesting at wavevectors near $\mathbf{k} = (\pi, \pi, 0)$.

The Bi $6p$ orbitals are spatially extended and strongly hybridized with S $3p$ states near the Fermi energy. Thus we do not expect electronic correlations to be essential for this compound. To check whether the conventional electron-phonon mechanism can be responsible for superconductivity here, we first perform a linear response phonon calculation [20] as implemented in QE[19]. An $18 \times 18 \times 6$ grid was used for the integration over IBZ. Our calculated phonon spectrum along major high symmetry lines of the Brillouin zone is shown in Fig.4 where the phonon dispersions are seen to extend up to 400 cm^{-1} . The phonon modes have only a little dispersion along Γ -Z direction, which again indicates the smallness of the interlayer coupling. There are basically three panels in the phonon spectrum that are easily distinguished along the Γ -Z direction. The top four branches above 300 cm^{-1} are mainly contributed by O and F, while the branches below 80 cm^{-1} come from the BiS_2 layer. The phonon vibrations within the xy -plane show a significant dispersion as shown in Fig.4. Analyzing the evolution of the phonon eigenvectors in the Brillouin zone reveals that there is clear separation between the xy and z polarized vibrations, and most of the modes show a definite in-plane or out-of-plane character.

A striking feature of this phonon spectrum is the presence of phonon softening around the M point that we associate with the strong Fermi surface nesting. We find that there are four totally unstable modes, mainly contributed by the S1 in-plane vibrations, where they either displace along x or y direction, and either in-phase or out-of-phase between the two BiS planes. The polarization vectors are shown in Fig.1b.

To understand whether the CDW instability is present in this material, we perform a frozen phonon analysis with the unit cell doubled ($\sqrt{2} \times \sqrt{2} \times 1$) according to the $(\pi, \pi, 0)$ nesting wave vector. We perform four calcu-

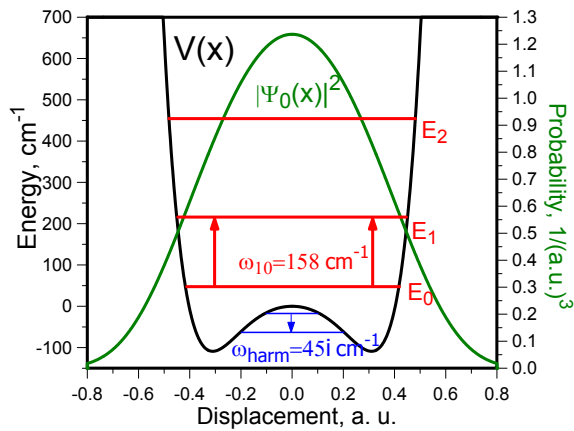


FIG. 5: Calculated double well potential for the unstable phonon mode using the frozen phonon method and its first three eigenstates.

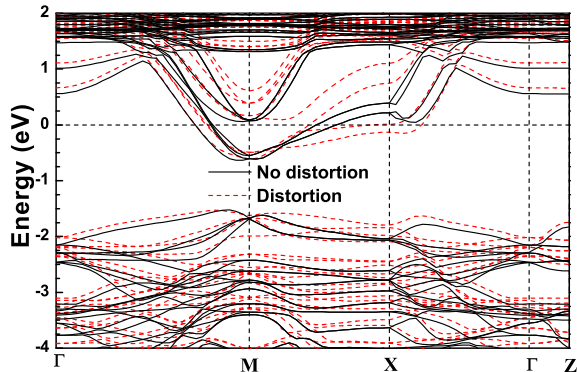


FIG. 6: Calculated band structure. Black line is the undistorted bands, red line is a distorted bands corresponding to the S1 in-plane displacement. See text for details.

lations by moving the atoms according to the eigenvectors of the four unstable phonon modes at the M point. Our frozen phonon calculations show a shallow double well potential where the S1 atoms shift about 0.18 Å away from the original high symmetry position as we show in Fig.5. To illustrate the crucial change in the electronic structure due to M point frozen phonon S1 in-plane motion, we show in Fig. 6 the band structures of distorted and undistorted structures in the vicinity of the Fermi level. The black lines depict the undistorted energy bands while the red lines correspond to the frozen-phonon distorted structure with S1 displacement by 0.18 Å. For comparison, both lines are drawn in an $\sqrt{2} \times \sqrt{2} \times 1$ supercell. A considerable difference in band structures induced by the in-plane S1 displacement indicates a large electron-phonon coupling from this CDW instability.

The depth of the double well is only about 100 cm^{-1} indicates that the displacements are dynamic. By solving a corresponding anharmonic oscillator problem we deduce a ground state atomic wave function which is in-

stead centered at the high symmetry position as shown in Fig. 5 together with the first three energy levels. It is therefore clear that our unstable modes are not related to a statically distorted structure of $\text{LaO}_{0.5}\text{F}_{0.5}\text{BiS}_2$. This is consistent with experimental observations that the resistivity changes smoothly from 300 K to about 10 K where the superconductivity occurs[1, 12].

We finally turn our discussion to the wave-vector (\mathbf{q}) and mode (ν) dependent electron-phonon coupling $\lambda_\nu(\mathbf{q})$. At first, this can be done for all stable phonons. Calculation shows that the O/F modes have negligible contribution to electron-phonon coupling. With strong hybridization, the coupling, however, is relatively strong for the BiS based modes. For example, we can find λ 's of the order of 1 for the S2 based optical phonons around 310 cm^{-1} near the Γ point. The analysis of the polarization vectors shows that these vibrations involve S2 movements towards Bi atoms. Unfortunately, finding the integral value of λ is a challenging problem due to the appearance of the imaginary frequencies, although neglecting completely the unstable modes results in already large average coupling constant (0.75) calculated using $4 \times 4 \times 2$ q-mesh. This is mainly due to the discussed S1/S2 vibrations.

To find the contribution for the four anharmonic modes, we follow the strategy of Ref. [25], where transitions from the ground to all phonon excited states of the anharmonic well need to be taken into account. The detailed theory using total energy frozen phonon method has been elaborated in Ref. [26]. Our numerical value of λ for the four anharmonic modes at the M point is 0.4. It has to be weighted somewhat by the area of the Brillouin Zone where the actual instability occurs therefore adding it the result for harmonic λ should give us a total coupling constant of 0.85. Inserting this value into the McMillan formula for T_c , with the Coulomb parameter $\mu^* \simeq 0.1$ and $\omega_D = 260K$ yields values of $T_c \simeq 11.3 K$ in reasonable agreement with experiment.

Finally, we have also performed calculations to check the effect of SOC, and show the results in the Supplemental Material. As can be seen from the Supplemental Material, the optimization including SOC gives very similar lattice parameters and internal atomic coordinates as those without SOC. We find that SOC does affect the band structure a little, but it does not change the Fermi surface. As shown in the Fig.S2 of Supplemental Material, the Fermi surface nesting does not disappear in the presence of SOC. Moreover, the CDW instability also remains to be active, as shown in the Fig.S3 of Supplemental Material. The band calculation with SOC also shows that S1 in-plane motion has a large effect on the band structure, same as the case without SOC (Fig. S4 of Supplemental Material), indicating strong electron-phonon coupling. The large electron-phonon coupling can be also found from the comparison of band structure from theoretical structure and experimental structure (Fig. 5S of

Supplemental Material).

In conclusion, electronic structure, lattice dynamics and electron–phonon interaction of the newly found superconductor $\text{LaO}_{0.5}\text{F}_{0.5}\text{BiS}_2$ have been investigated using density functional theory and linear response approach. A strong Fermi surface nesting at $(\pi, \pi, 0)$ results in large phonon softening and strongly anharmonic double well behavior of the total energy as a function of the in-plane S displacements. A large electron–phonon coupling constant $\lambda=0.85$ is predicted, which emphasizes that $\text{LaO}_{0.5}\text{F}_{0.5}\text{BiS}_2$ is a strongly coupled electron–phonon superconductor.

X.G.W acknowledge useful conversations with Prof. H.H. Wen, J. X. Li and Q.H. Wang. The work was supported by the National Key Project for Basic Research of China (Grants No. 2011CB922101 and No. 2010CB923404), NSFC under Grants No. 91122035, 11174124, 10974082, 61125403 and 50832003), PAPD, PCSIRT, NCET. Computations were performed at the ECNU computing center. S.Y.S was supported by by DOE Computational Material Science Network (CMSN) Grant No. DESC0005468.

-
- [1] W. E. Pickett, Rev. Mod. Phys. **61**, 433 (1989).
 [2] Y. Maeno, H. Hashimoto, K. Yoshida, S. Nishizaki, T. Fujita, J. G. Bednorz and F. Lichtenberg, Nature **372**, 532 (1994).
 [3] J. Nagamatsu, N. Nakagawa, T. Muranaka, Y. Zenitani, and J. Akimitsu, Nature **410**, 63 (2001).
 [4] Y. Kamihara, T. Watanabe, M. Hirano, and Hideo Hosono, J. Am. Chem. Soc. **130**, 3296 (2008).
 [5] J. Paglione and R. L. Greene, Nature Phys. **6**, 645 (2010).
 [6] J. Dong, H. J. Zhang, G. Xu, Z. Li, G. Li, W. Z. Hu, D. Wu, G. F. Chen, X. Dai, J. L. Luo, Z. Fang and N. L. Wang, Europhys. Lett. **83**, 27006 (2008).
 [7] Y. Mizuguchi, H. Fujihisa, Y. Gotoh, K. Suzuki, H. Usui, K. Kuroki, S. Demura, Y. Takano, H. Izawa and O. Miura, arXiv:1207.3145 (2012).
 [8] Y. Mizuguchi, S. Demura, K. Deguchi, Y. Takano, H. Fujihisa, Y. Gotoh, H. Izawa and O. Miura, arXiv:1207.3558 (2010).
 [9] S. Demura, Y. Mizuguchi, K. Deguchi, H. Okazaki, H. Hara, T. Watanabe, S. J. Denholme, M. Fujioka, T. Ozaki, H. Fujihisa, Y. Gotoh, O. Miura, T. Yamaguchi, H. Takeya and Y. Takano, arXiv:1207.5248 (2012).
 [10] S. Li, H. Yang, J. Tao, X. Ding and H.H. Wen, arXiv:1207.4955 (2012).
 [11] S. G. Tan, L. J. Li, Y. Liu, P. Tong, B. C. Zhao, W. J. Lu, Y. P. Sun, arXiv:1207.5395.
 [12] H. Kotegawa, Y. Tomita, H. Tou, H. Izawa, Y. Mizuguchi, O. Miura, S. Demura, K. Deguchi and Y. Takano, arXiv:1207.6935 (2012).
 [13] H. Usui, K. Suzuki and K. Kuroki, arXiv:1207.3888 (2012).
 [14] T. Zhou and Z. D. Wang, arXiv:1208.1101 (2012).
 [15] V. P. S. Awana, Anuj Kumar, Rajveer Jha, Shiva Kumar, Jagdish Kumar, Anand Pal, Shruti, J. Saha, S. Patnaik,

TABLE II: The numerical Wyckoff positions of $\text{La}(\text{O}_{0.5}\text{F}_{0.5})\text{BiS}_2$ based on the experimental lattice parameter. Experimental Wyckoff positions [1] are also listed for comparison.

La(O _{0.5} F _{0.5})BiS ₂		
Site	Cal.	Exp.
z La (2b)	0.1064	0.1015
z Bi (2b)	0.6149	0.6231
z S1 (2b)	0.3838	0.3657
z S2 (2b)	0.8137	0.8198
z O (2a)	0.0000	0.0000
z F (2a)	0.0000	0.0000

- arXiv:1207.6845 (2012).
 [16] S. K. Singh, A. Kumar, B. Gahtori, Shruti, G. Sharma, S. Patnaik, V. P. S. Awana, arXiv:1207.5428 (2012).
 [17] J. P. Perdew, K. Burke, and M. Ernzerhof, Phys. Rev. Lett. **77**, 3865 (1996).
 [18] G. Kresse and J. Furthmuller, Comput. Mater. Sci. **6**, 15 (1996); G. Kresse and J. Furthmuller, Phys. Rev. B **54**, 11169 (1996).
 [19] P. Giannozzi *et al.*, J. Phys.: Condens. Matter, **21**, 395502 (2009).
 [20] S. Baroni, S. de Gironcoli, A. Dal Corso, and P. Giannozzi, Rev. Mod. Phys. **73**, 515 (2001).
 [21] Z. P. Yin, S. Lebegue, M. J. Han, B. P. Neal, S. Y. Savrasov, and W. E. Pickett, Phys. Rev. Lett. **101**, 047001 (2008).
 [22] V. Meregalli and S. Y. Savrasov, Phys. Rev. B **57**, 14453 (1998).
 [23] P. B. Allen, Phys. Rev. B **6**, 2577 (1972).
 [24] S.Y. Savrasov, Phys. Rev. Lett. **69**, 2819 (1992); S.Y. Savrasov, D.Y. Savrasov, and O.K. Andersen, Phys. Rev. Lett. **72**, 372 (1994).
 [25] J.C.K. Hui, and P.B. Allen, J. Phys. F: Met. Phys. **4**, L42 (1974).
 [26] V. Meregalli and S. Y. Savrasov, Phys. Rev. **57**, 14453 (1998).

SUPPLEMENTARY MATERIAL

We have optimized all independent internal atomic coordinates based on the experimental lattice parameter, and show the obtained results in Table 1S. Note here for consistency, the results shown in Supplementary Material are all obtained using Vienna Ab–Initio Simulation Package (VASP). As can be seen from the Table 1S, the inter-layer distance has only small effect on the discrepancy between theoretical and experimental z -coordinates of S1 atom.

To study the influence of spin-orbit coupling (SOC), we have also performed the calculation including SOC. The optimized lattice parameters and Wyckoff positions of $\text{La}(\text{O}_{0.5}\text{F}_{0.5})\text{BiS}_2$ are shown in Table 2S. For comparison, we also list the corresponding values from the calculation without SOC in Table 2S. It is found that the

TABLE III: Lattice parameters and Wyckoff positions of $\text{La}(\text{O}_{0.5}\text{F}_{0.5})\text{BiS}_2$ from the calculation with and without SOC.

	Site	without SOC	with SOC
a (Å)	–	4.0782	4.0781
c (Å)		13.4835	13.4566
z	La (2b)	0.1055	0.1051
z	Bi (2b)	0.6161	0.6163
z	S1 (2b)	0.3891	0.3831
z	S2 (2b)	0.8154	0.8149
z	O (2a)	0.0000	0.0000
z	F (2a)	0.0000	0.0000

SOC has only very small effect on the lattice structure of $\text{La}(\text{O}_{0.5}\text{F}_{0.5})\text{BiS}_2$. Comparing with the results without SOC from QE (Table I in the manuscript) shows the consistency of VASP and QE is satisfactory.

We show the band structure with and without the SOC in Fig. 1S. As can be seen from Fig. 1S, the SOC has a considerable effect on the bands around X point. To be specific, there are four bands crossing the Fermi level in the band structure without SOC, whereas including SOC pushes two bands above the Fermi level. Nevertheless, it is very interesting to notice that the Fermi surface from SOC calculation is still quite similar to that without SOC (see Fig. 2S). As shown in Fig. 2S, including SOC does not change the two dimensional-like feature of the Fermi surface. Moreover, the strong Fermi surface nesting can still be found at wavevectors near $k = (\pi, \pi, 0)$, as shown in Fig. 2S(b), and the main effect of SOC is to eliminate a small pocket around X point.

To check the effect of SOC on the CDW instability, we also perform four SOC calculations by moving the atoms according to the eigenvectors of the four unstable phonon modes at the M point. Our frozen phonon calculations show that the double well potential remains, though the well-depth drops considerably, as shown in Fig. 3S.

We show in Fig. 4S the band structures of distorted and undistorted structures due to M point frozen phonon S1 in-plane motion in the vicinity of the Fermi level. Same with the calculation without SOC, considerable difference in band structures induced by the in-plane S1 displacement which again indicates a large electron-phonon coupling from this CDW instability. The large electron-phonon coupling can be also found from the comparison of band structure from theoretical structure and experimental structure as shown in Fig. 5S.

As a final comment, we recall that the calculation without SOC is found for heavy element Pb to be satisfactory [2] therefore we do not foresee significant changes in our

estimation of the electron-phonon interaction when the SOC effect is taken into account.

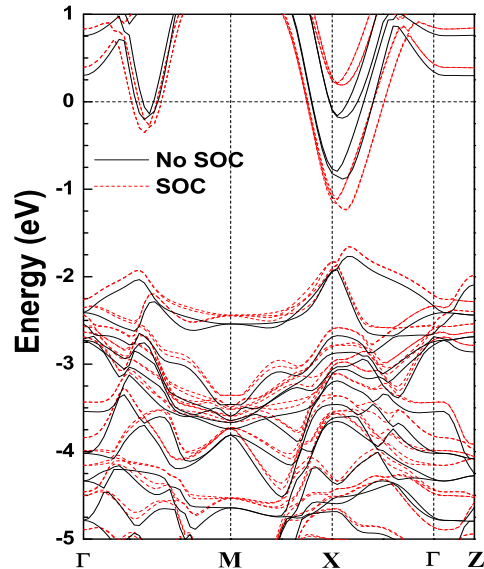


FIG. S1: Band structure plot

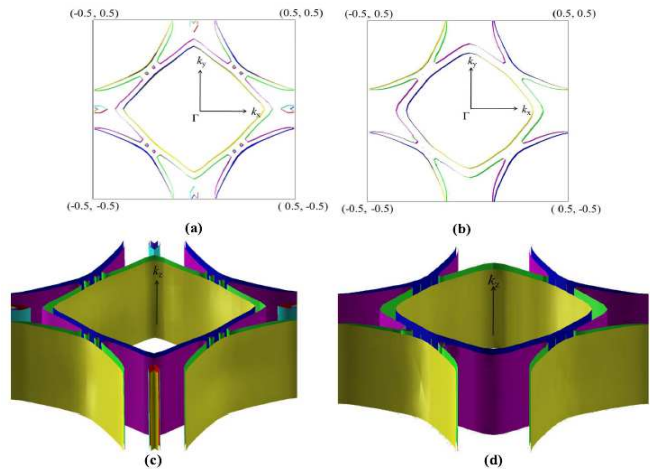


FIG. S2: Fermi surface of $\text{La}(\text{O}_{0.5}\text{F}_{0.5})\text{BiS}_2$ cross section for $k_x=0$: (a) without SOC, (b) with SOC and 3D view: (c) without SOC, (d) with SOC.

-
- [1] Y. Mizuguchi, S. Demura, K. Deguchi, Y. Takano, H. Fujihisa, Y. Gotoh, H. Izawa and O. Miura, arXiv:1207.3558 (2012).
 [2] S. Y. Savrasov and D. Y. Savrasov, Phys. Rev. B 54, 16487 (1996).

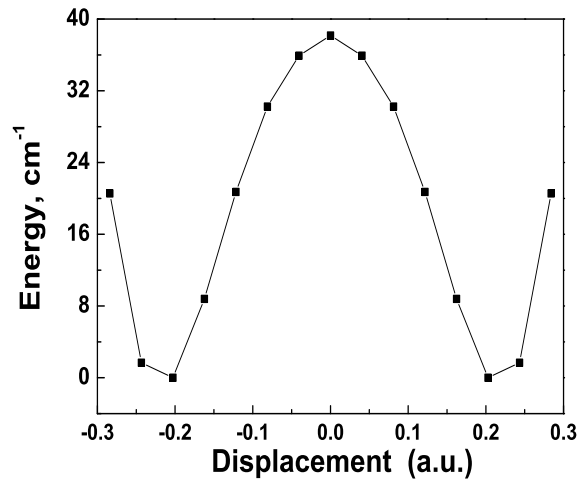


FIG. S3: Double well potential for the unstable phonon mode using the frozen phonon method from the calculation with SOC.

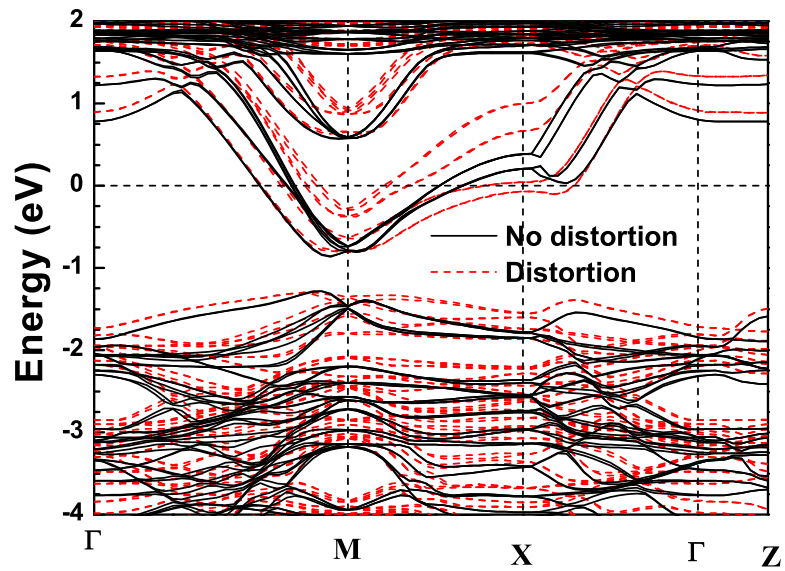


FIG. S4: Band structure from calculation with SOC. Black line is the undistorted bands, red line is a distorted bands corresponding to the S1 in-plane displacement.

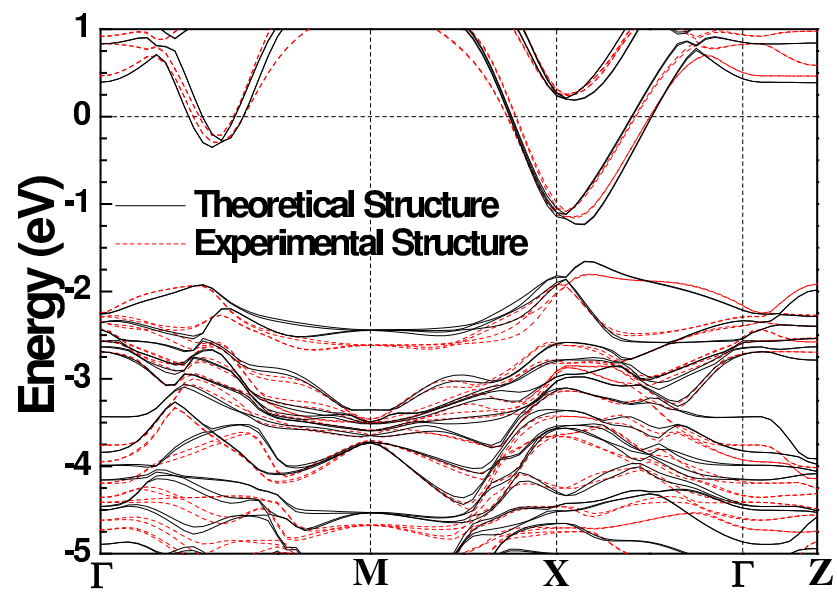


FIG. S5: Band structure from the calculation with SOC.